

## Sulfite-oxidizing enzymes

Ulrike Kappler · John H. Enemark

Received: 28 July 2014 / Accepted: 15 September 2014 / Published online: 27 September 2014  
© SBIC 2014

**Abstract** Sulfite-oxidizing enzymes (SOEs) are molybdenum enzymes that exist in almost all forms of life where they carry out important functions in protecting cells and organisms against sulfite-induced damage. Due to their nearly ubiquitous presence in living cells, these enzymes can be assumed to be evolutionarily ancient, and this is reflected in the fact that the basic domain architecture and fold structure of all sulfite-oxidizing enzymes studied so far are similar. The Mo centers of all SOEs have five-coordinate square pyramidal coordination geometry, which incorporates a pyranopterin dithiolene cofactor. However, significant differences exist in the quaternary structure of the enzymes, as well as in the kinetic properties and the nature of the electron acceptors used. In addition, some SOEs also contain an integral heme group that participates in the overall catalytic cycle. Catalytic turnover involves the paramagnetic Mo(V) oxidation state, and EPR spectroscopy, especially high-resolution pulsed EPR spectroscopy, provides detailed information about the molecular and

electronic structure of the Mo center and the Mo-based sulfite oxidation reaction.

**Keywords** Sulfite oxidation · Electron transfer · Electron paramagnetic resonance · Molybdenum enzyme · Pyranopterin dithiolene

### Abbreviations

CSO	Chicken sulfite oxidase
CW EPR	Continuous wave electron paramagnetic resonance
Cyt <i>c</i>	Cytochrome <i>c</i>
DFT	Density functional theory
ESE	Electron spin echo
ESEEM	Electron spin echo envelope modulation
HSO	Human sulfite oxidase
IET	Intramolecular electron transfer
PPT	Pyranopterin dithiolene
PSO	Plant sulfite oxidase
SDH	Sulfite dehydrogenase
SO	Sulfite oxidase
SOE	Sulfite-oxidizing enzyme
SorAB	SorAB sulfite dehydrogenase from <i>Starkeya novella</i>
SorT	SorT sulfite dehydrogenase from <i>Sinorhizobium meliloti</i>
SorU	<i>c</i> -type cytochrome, natural electron acceptor for SorT
SUOX	Sulfite oxidase

Responsible Editors: José Moura and Paul Bernhardt.

**Electronic supplementary material** The online version of this article (doi:10.1007/s00775-014-1197-3) contains supplementary material, which is available to authorized users.

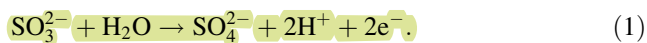
U. Kappler (✉)  
Centre for Metals in Biology, School of Chemistry and  
Molecular Biosciences, The University of Queensland, St. Lucia,  
QLD 4072, Australia  
e-mail: u.kappler@uq.edu.au

J. H. Enemark  
Department of Chemistry and Biochemistry, University of  
Arizona, Tucson, AZ 85721-0041, USA  
e-mail: jenemark@email.arizona.edu

### Introduction

Sulfite-oxidizing enzymes (SOEs) are molybdenum-containing enzymes that occur in bacteria, plants and

vertebrates. These enzymes catalyze the oxidation of sulfite to sulfate with the concomitant release of two protons and two electrons, Eq. (1).



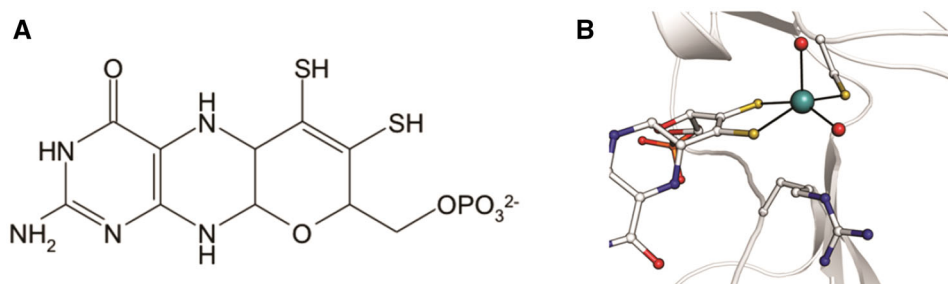
An interesting feature of this reaction is that water is the source of the oxygen that is incorporated into the substrate (sulfite), not dioxygen, as occurs for oxidases with metals other than molybdenum at their catalytic center [1]. This review focuses on how the chemistry of Eq. (1) is embedded in quite different physiological contexts in bacteria, plants and vertebrates, and how the terminal acceptor for the electrons generated by Eq. (1) differs for each class of organism. In most cases, these enzymes appear to be required to protect cells from sulfite-induced damage, although both the vertebrate and bacterial enzymes also contribute to cellular energy generation by transferring electrons to cytochrome oxidase [2, 3]. A comprehensive review of all mononuclear molybdenum enzymes, including SOEs, recently appeared [4].

In bacteria SOEs occur in a variety of species many of which can oxidize either inorganic or organic sulfur compounds to generate energy for growth (e.g., *Starkeya novella*, *Sinorhizobium meliloti*, *Thermus thermophilus* or *Cupriavidus necator* [5–8]), but SOEs are also found in bacteria where this type of sulfur metabolism is not known (e.g., *Campylobacter jejuni* [9]). SOE activity in bacteria was already reported in the 1960s, but the first enzyme purification and characterization were only reported in 2000 [6, 10, 11]. Since then, several bacterial SOEs have been purified or produced using heterologous expression systems, and several of these enzymes are known to have different quaternary structures [5–9, 12]. The general cellular location of the bacterial SOEs is the periplasm, and where identified, the natural electron acceptors of these enzymes appear to be *c*-type cytochromes [6, 13, 14]. Where *c*-type cytochromes are used as external electron acceptors for SOEs, these electrons can be fed into the respiratory chain at the level of the cytochrome oxidase, leading to energy conservation. However, the energy yields from this reaction are low, and usually sulfite oxidation alone will not support cell growth.

Plant sulfite oxidase (PSO) was first identified in *Arabidopsis thaliana* in 2001 [15]. The gene for this protein is highly conserved in the plant kingdom, being found in higher plants, algae and mosses. PSO is localized in the peroxisome, so the function of PSO is not related to the chloroplast-based sulfur assimilation pathway [16]. Rather, the function of PSO is to remove toxic sulfite generated during the decomposition of sulfur-containing amino acids and excess sulfite derived from SO<sub>2</sub> gas in the atmosphere [17]. Oxygen is the terminal electron acceptor for Eq. (1) for PSO, with the final product being hydrogen peroxide. However, extensive studies of the kinetics of this reaction show that nearly all of the O<sub>2</sub> consumed in the reoxidation of PSO is initially converted to superoxide while hydrogen peroxide is only subsequently produced via a spontaneous, non-enzymatic dismutation reaction [18].

Vertebrate SOs are soluble enzymes found in the intermembrane space of mitochondria. They are expressed at low levels in almost all body tissues, but occur in high concentrations in the liver [19]. Cytochrome *c* (cyt *c*) is the physiological electron acceptor for Eq. (1). In humans, oxidation of toxic sulfite to sulfate is the final step in the catabolism of the sulfur-containing amino acids cysteine and methionine [20]. Human sulfite oxidase (HSO) also functions in detoxifying sulfite exogenously obtained from environmental and dietary sources and from the metabolism of sulfur-containing xenobiotics. Sulfite oxidase deficiency is an inherited recessive genetic disease that causes severe neonatal neurological problems, including dislocation of the ocular lenses, attenuated growth of the brain, mental retardation [21, 22], seizures [23] and often early death. General sulfite oxidase deficiency is caused by the inability to biosynthesize the pyranopterin dithiolene cofactor, abbreviated PPT in this review (Fig. 1a), which coordinates to the Mo atom (MoPPT) as part of the five-coordinate square pyramidal active site common to all SOEs (Fig. 1b). This cofactor has also been called “molybdopterin” or MPT [24]. The history of the discovery of this cofactor and the elucidation of its biosynthetic pathways in bacteria and higher organisms have been described [24, 25]. Isolated sulfite oxidase deficiency results from certain

**Fig. 1** **a** Schematic representation of the Pyranopterin (PPT) cofactor. **b** Square pyramidal structure of the SOE active sites. Image shows the active site of the SorT SDH from *S. meliloti* [40]



point mutations in the HSO protein [26] (see Supplementary Material).

### Structures of SOEs

All SOEs described above belong to the same enzyme family, the sulfite oxidase (SO) superfamily of molybdoenzymes (cd00321, COG2041). In addition to SOEs, the SO family also contains the plant nitrate reductases as well as several bacterial and archaeal enzymes of unknown function (cd groups 02107-02114). The proteins that belong to the SO enzyme family can be subdivided into three main groups that have different basic domain structures (Fig. 2) [2, 27], but despite these differences, all SO

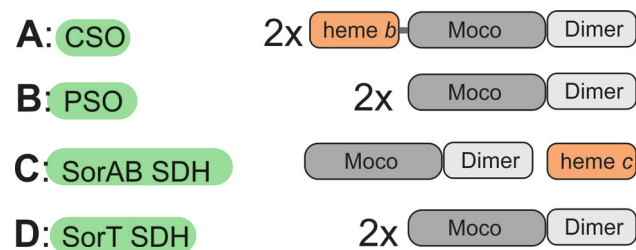
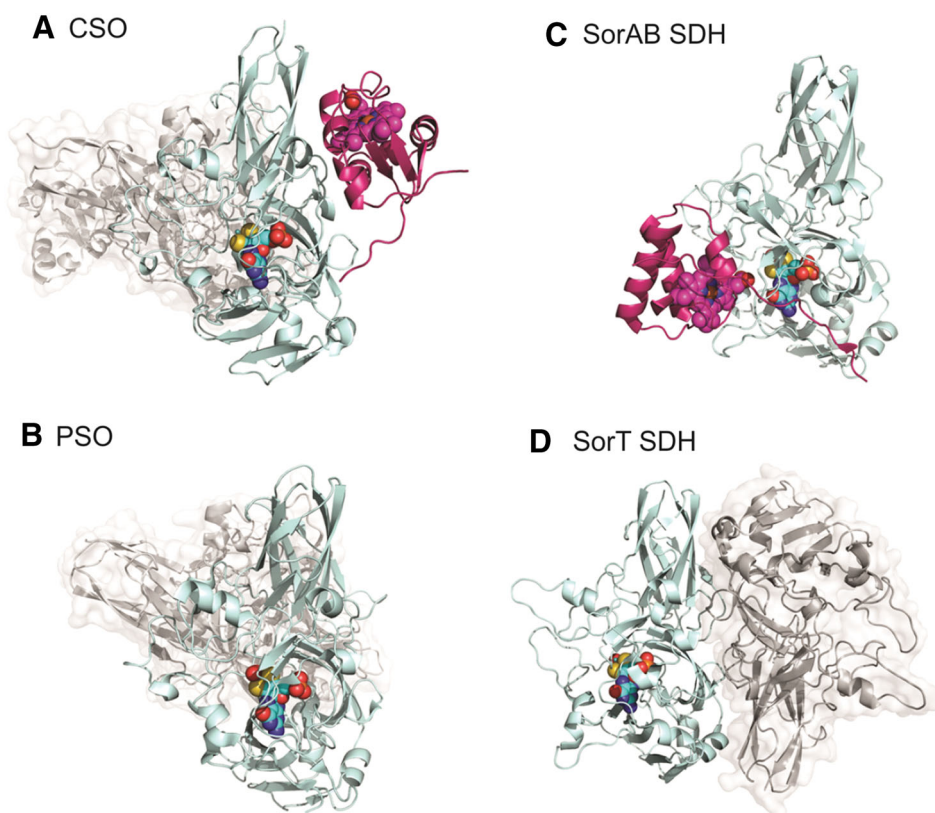


**Fig. 2** Schematic representation of the domain structure of sulfite-oxidizing enzymes (SOEs). Moco MoPPT binding domain, dimer dimerization domain, heme b/c b- or c-type heme binding domains or subunits, 2x protein is a dimer of the subunit shown

**Fig. 3** X-ray crystal structures of SOEs from vertebrates, plants and bacteria. CSO chicken liver sulfite oxidase [31], PSO plant sulfite oxidase [29], SorAB SDH SorAB sulfite dehydrogenase from *Starkeya novella* [37], SorT SDH SorT sulfite dehydrogenase from *Sinorhizobium meliloti* [40]. MoPPT and dimerization domains are shown in cyan, the MoPPT cofactor is shown as a space fill representation. In structures a, c, the heme domains are shown in purple



family enzymes for which structures have been solved share the basic fold of the Mo-containing domain, the so-called SUOX-fold which consists of three antiparallel and one mixed beta sheet, six alpha-helices and four  $3_{10}$  helices (Fig. 3) [28]. The MoPPT binding domain is the central part of these enzymes as it contains the active site, but additional functional domains may be present. For SOEs, the second key domain is the dimerization domain which is found in all enzymes of the SO family that are known to oxidize sulfite. The dimerization domain also has a conserved fold that consists mainly of two elongated beta-sheets that contain a Greek key motif [28, 29], and its name refers to the fact that it mediates the majority of the homodimer interactions in CSO- and PSO-type enzymes. This domain appears to have no primary involvement in catalysis/enzyme function, although some mutagenesis studies carried out using HSO showed reduced catalytic performance of HSO variants carrying mutations that map to the dimerization domain [30].

Despite the similarities of the basic structural domains present in the characterized SOEs, the actual quaternary structures of CSO, PSO and the bacterial enzymes differ significantly.

The first SOE for which a structure was solved was chicken liver sulfite oxidase (CSO) (Fig. 3a) [31]. HSO and CSO have 68 % sequence identity (85 % sequence similarity), so the structure of CSO is a good template for

discussing HSO, whose structure is not known. In addition to the MoPPT binding domain and the dimerization domain, CSO also contains a heme *b* binding domain which is linked to the core structure of the MoPPT and dimerization domains by a flexible linker of  $\sim 10$  amino acids (residues 85–95). So overall, CSO- and HSO-type SOEs contain a Mo and a heme redox center in each subunit. It has long been recognized that the latter domain is mobile [32], and it was also shown that it can be removed from the main body of the enzyme by proteolytic cleavage [33, 34]. Separation of the heme domain from the Mo domain is possible because the flexible linker region by which the domain is connected to the main body of the enzyme is accessible to proteases and separation of the domains results in loss of electron transfer from the SOE to cytochrome *c*. However, the isolated Mo domain remains catalytically competent in assays using the artificial electron acceptor ferricyanide [34]. During catalysis, the mobile heme domain is thought to reposition itself, so that it can accept electrons from the Mo redox center [35], and in fact the length of the linker is a key feature for efficient catalysis in HSO [36].

The crystal structure of the CSO clearly revealed the homodimeric structure of the enzyme with all three domains being resolved (Fig. 3a), however, the heme *b*-containing domain was located away from the Mo active site, with a Mo to Fe distance of 32.3 Å that would not allow for efficient electron transfer. The overall dimensions of the enzyme were  $120 \times 50 \times 77 \text{ Å}^3$ , and interactions between the two subunits were mediated mostly by residues in the dimerization domain [31]. The total buried surface area between the two subunits of CSO is 8.5 % (or  $1,573 \text{ Å}^2$ ) of each monomer's surface area and interactions involve 30 hydrogen bonds and salt bridges. The Mo active site was found buried deeply in the MoPPT domain, with a single PPT cofactor, a cysteine residue (Cys185), one oxo and a hydro ligand coordinating the Mo ion in a square pyramidal conformation (Fig. 1b) [31]. Three conserved arginine residues were identified in the substrate access channel leading to the Mo active site, with one arginine each being located at the entrance to the channel (Arg450), part way along the channel (Arg190) and next to the Mo ion (Arg138). The positive charges of the arginine residues complement the negative charges on the enzyme's substrate, sulfite, and were thus suggested to be involved in substrate binding. In fact, a sulfate molecule was present in the CSO active site. In addition to the Arg138 residue, a tyrosine (Tyr322) was found in hydrogen bonding distance to the equatorial hydro ligand of the Mo center [31].

The structure of plant sulfite oxidase (source: *Arabidopsis thaliana*, PSO) which was solved in 2003 (Fig. 3b) [29] showed a structure very similar to that of CSO

(Fig. 3a). PSO does not contain a heme domain, but it is a homodimeric enzyme with overall dimensions of  $69 \times 59 \times 48 \text{ Å}^3$  [29]. Each monomer contains the MoPPT domain and a dimerization domain, and interactions between the two dimers are mediated mostly by residues in the dimerization domain, burying approx. 10 % (or  $1,690 \text{ Å}^2$ ) of each monomer's surface area. The interactions between the subunits are stabilized by 20 hydrogen bonds. Again, the Mo active site was well resolved and the conserved arginine residues were identified in the substrate access channel.

The relative orientation of the PSO monomers in the dimer is slightly different from that seen in CSO, leading to 1.85 Å rms deviation in an overlay of the two structures.

While the basic structures of CSO and PSO are very similar both in the domain architecture and the way in which the monomers interact, the structure of the first bacterial SOE, the SorAB sulfite dehydrogenase from *Starkeya novella*, revealed a different quaternary structure (Fig. 3c) [37]. The SorAB SDH is a heterodimer composed of a catalytic subunit (SorA) with the familiar domain architecture (MoPPT and dimerization domain) and a small *c*-type cytochrome, SorB (Fig. 3b). SorB is an integral part of the enzyme and cannot be removed from the complex without destroying the enzyme activity. The SorAB subunits form a heterodimer with a buried surface area of  $2,800 \text{ Å}^2$ . Interactions between the two subunits involved 30 direct hydrogen bonds and two salt bridges between residues on the two sides of the interface. An N-terminal extension of SorB was found to wrap around the SorA subunit [37].

In addition to this very different quaternary structure of this SOE, the SorAB crystal structure allowed insights into interactions between the Mo and heme redox cofactors. In the SorAB complex the two cofactors approach to a distance of 16.6 Å (Mo–Fe), with the edge-to-edge distance of the redox cofactors being even closer, only 8.5 Å [37]. The basic structure of the Mo site (Fig. 1b) is the same as in CSO and PSO. A hydrogen bonding network connects the two redox centers present in SorAB, with one of the conserved arginine residues (Arg55, equivalent to Arg138 in CSO) in the substrate access channel forming hydrogen bonds with both the equatorial hydro group on the Mo center and one of the heme propionate groups [37]. It would appear that the mode of interactions between a heme and a MoPPT center of an SOE is well conserved as it has been shown that the CSO heme *b* domain could be modeled in a position very similar to that of SorB in the SorAB complex [38], and while SorB and the heme *b*<sub>5</sub> domain of CSO are structurally unrelated, both proteins show a similar solvent exposure of the heme cofactor near the site where the heme/Mo interactions occur [37]. In addition, in the permanent SorAB complex, the SorB heme is also

solvent exposed at a second site which has been proposed to be the site where interactions of SorAB with an external electron acceptor occur [37].

Although SorAB was the first bacterial SOE for which a crystal structure became available, this enzyme does not appear to be a key representative of bacterial SOEs [2]. Since the purification of the SorAB enzyme from *S. novella*, at least six other bacterial SOEs have been purified and at least partially characterized, and only one of these enzymes might contain a heme redox center as an integral part of the enzyme [2]. Instead, most of the bacterial enzymes appear to be homodimers (with one enzyme being reported to also exist as a monomer) that contain only Mo redox centers [2], i.e., these enzymes might be expected to have structures similar to that of PSO. An interesting feature of these bacterial SOEs is that several of them appear to have an unusual domain packing, as on gel filtration columns they elute at position corresponding to a molecular mass of approx.  $\sim 1.5$  monomers [2, 7, 8, 39], although Multi-Angle Laser Light Scattering (MALLS) analysis was able to correctly size one of the proteins as a homodimer [7].

A possible reason for this is apparent in the recently solved crystal structure of the SorT SOE from *Sinorhizobium meliloti* [40]. While the basic domain and protein fold structure of each of the SorT monomers are very similar to those of the other three enzymes, the packing of the monomers is unlike any that has been seen before. Unlike the CSO and PSO homodimers where subunit interactions are mostly mediated by residues in the dimerization domain, the SorT monomers interact in an ‘upside down’ fashion, where each dimerization domain interacts with the MoPPT domain of the other subunit (Fig. 3d). This type of domain packing had not been previously observed for any SOE, but it seems likely that several of the bacterial SOEs that also show unusual gel filtration properties might have similar quaternary structures.

Despite this difference in the arrangement of the monomers, the SorT active site shows the familiar square pyramidal geometry [40], and the enzyme has been shown to use an external *c*-type cytochrome (SorU) as its electron acceptor [13].

In summary, the SOE crystal structures all share the domain structure and fold of the main catalytic subunit which contains a single Mo active site per catalytic subunit (Fig. 1b). The total number and type of redox centers present in each enzyme, however, differ significantly, as does the arrangement of the subunits in the enzymes. In particular, the two SOEs that contain heme domains differ considerably in the way in which these additional redox centers have been incorporated into the enzymes. The heme domain of CSO-type enzymes is part of the main catalytic subunit of the enzyme, but retains mobility due to

the presence of a flexible tether/linker region, while in the bacterial SorAB SDH the heme-containing SorB subunit is not physically linked to the catalytic subunit, SorA, but forms a permanent complex with it.

Another interesting feature of SOEs is that at present the available crystal structures do not allow definite predictions about the preferred electron acceptors used by each SOE. While the two bacterial enzymes are not able to transfer electrons to oxygen and thus are sulfite dehydrogenases, the vertebrate SOEs (CSO, HSO) are able to transfer electrons to both cytochrome *c* (preferred electron acceptor) and molecular oxygen, while PSO appears to interact exclusively with molecular oxygen as the electron acceptor. This is even more puzzling as the Mo active sites of all four types of SOEs are strikingly similar (Fig. 1b), and any argument proposing that the absence of a heme subunit/domain close to the catalytic subunit would allow the enzyme to interact with oxygen does not hold true in view of the structure of SorT, which has the same relatively ‘open’ active site that is found in PSO and CSO, but for which so far no activity with molecular oxygen as the electron acceptor has been detected [7, 13].

The number of redox centers present in an SOE and the type of electron acceptor used have direct implications for its overall reaction mechanism, and the contributions of the different redox centers to the reaction are described below.

### Basic kinetic properties of SOEs from various sources

The kinetics of sulfite oxidation by SOEs have been investigated in detail using both steady-state and pre-steady-state kinetics, with many investigations focusing on CSO/HSO which were the first SOEs to be comprehensively characterized [5–7, 15, 18, 30, 41–49]. The pre-steady-state kinetics were essential in establishing the catalytic cycle of SOEs which will be discussed in more detail below.

Sulfite oxidation as described by Eq. (1) requires the transfer and transient storage of two electrons in the SOE, and the reaction cycle can be divided into a reductive and an oxidative part.

Figure 4 schematically illustrates the proposed overall catalytic cycle for SOEs that contain both a Mo center and a heme center. The oxidized, resting state shown in bold in the box at the top of the cycle is Mo(VI)/Fe(III). The reductive half of the reaction occurs at the molybdenum redox center, and the first step is likely to be similar for all SOEs described above. Sulfite is transiently bound to the equatorial oxo/hydroxyl ligand of the Mo center, leading to a two-electron reduction of the Mo center (from Mo(VI) to Mo(IV)) and oxidation of sulfite to sulfate, which is released through hydrolysis that involves water. In SOEs

with more than one integral redox center, a stable Mo(V) state is then formed when one of the two electrons stored in the Mo center is rapidly passed on to the second (heme) redox center [6, 41, 43, 46]. In CSO, the driving force for this intramolecular electron transfer reaction (IET#1) to form the Mo(V)/Fe(II) state (shown in bold in the box at the lower right of Fig. 4) is  $\sim 300$  mV [50], so the arrow in the forward direction for IET#1 in Fig. 4 is shown much larger than that in the reverse direction. This state is characterized by a change in the electronic spectrum of the heme domain and the appearance of distinctive Mo(V) EPR spectra (see below). Stopped-flow studies of

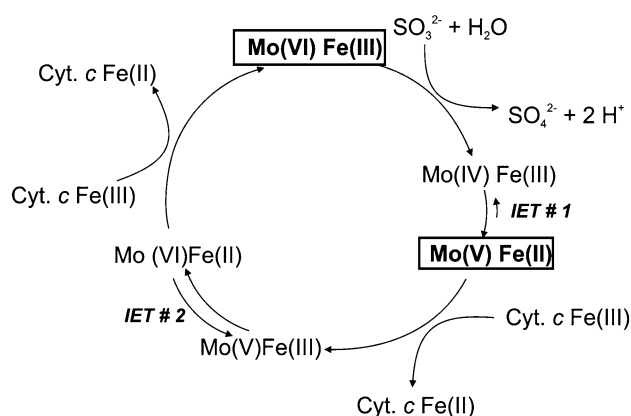


**Fig. 4** Schematic representation of the reaction cycle of heme-containing SOEs. *Cyt c* cytochrome *c*, *IET* intramolecular electron transfer. Mo and Fe denote the central metals in the two redox centers, Roman numerals in parentheses indicate the redox states of the metals, and the relatively stable oxidation states are shown in *dark boxes*. For plant sulfite oxidase (PSO), which does not have an integral heme center, molecular oxygen,  $O_2$ , is the one-electron acceptor via the general cycle of Fig. 5. Vertebrate SOs can also utilize  $O_2$  as the terminal electron acceptor (see text)

the reductive half-reaction for CSO show that  $k_{\text{red}} = 184 \text{ s}^{-1}$ , which is substantially faster than turnover ( $47 \text{ s}^{-1}$ ) [41] (Table 1).

In the oxidative part of the reaction cycle, the reduced SOEs undergo sequential one-electron transfers to an external electron acceptor (e.g., cytochrome  $c_{550}$ , SorU), leading to a restoration of the catalytically active Mo(VI) state of the SOE. In Fig. 4, two *cyt c* molecules are reduced in the oxidative part of each catalytic cycle. Some studies report  $k_{\text{cat}}$  as ‘per *cyt c* reduced’ [41], whereas others [46, 47] give the ‘turnover number/ $k_{\text{cat}}$  for sulfite’. In comparing kinetic data for SOEs, it is important to determine which method has been used and to realize that  $k_{\text{turnover}} = \frac{1}{2} k_{\text{cat}(\text{cyt } c)}$ . In Table 1, all of the steady-state data are given as turnover numbers for the oxidation of sulfite. The oxidative pathway of SOEs has also been studied by rapid kinetics experiments. For CSO,  $k_{\text{ox}} = 550 \text{ s}^{-1}$  at pH 8, much faster than either turnover or the reductive half-reaction. The conclusions from the extensive steady-state and rapid kinetics studies of CSO are that the first step in the reductive part of the catalytic cycle, i.e., the reaction of sulfite with the oxidized Mo(VI) center, is rate limiting above pH 7, and the subsequent electron transfer steps of the reductive and oxidative paths are much faster [41]. Kinetic studies of native CSO suggested that the conserved active site tyrosine (Y322) may play an important role in the reaction of the Mo center with sulfite [32] [41]. In HSO, the Y343F variant of the analogous tyrosine showed altered substrate binding and decreased catalytic activity, which was attributed to impaired product release from Mo(IV) prior to the ET steps [43]. For SorAB, the catalytic activity of the Y236F variant at pH 8 is only about 15 % of wt enzyme [46]. The effects of these

**Table 1** Kinetic properties of well-characterized SOEs

Enzyme properties	Vertebrate SOEs		Plant SOE PSO <i>A. thaliana</i>	Bacterial SOEs	
	CSO	HSO		SorAB <i>S. novella</i>	SorT <i>S. meliloti</i>
Subunit composition	$\alpha_2$	$\alpha_2$	$\alpha_2$	$\alpha\beta$	$\alpha_2$
Redox centers	Mo, heme <i>b</i>	Mo, heme <i>b</i>	Mo	Mo, heme <i>c</i>	Mo
Turnover number ( $\text{s}^{-1}$ , pH 8)	$47.5 \pm 1.9$	$25 \pm 1.27$	4,500	$345 \pm 11$	$343 \pm 11$
$K_m$ , sulfite ( $\mu\text{M}$ , pH 8)	$16.4 \pm 3$	$6.12 \pm 0.46$	$33.8 \pm 3.2$	$22 \pm 2.6$	$15.5 \pm 1.9$
pH optimum	8.5–9.0	8.0–9.0	n.r.	9.0	8.0–9.5
Electron acceptors	Cytochrome <i>c</i> , oxygen, ferricyanide	Cytochrome <i>c</i> , oxygen, ferricyanide	Oxygen, ferricyanide	Cytochrome <i>c</i> , ferricyanide	Cytochrome <i>c</i> , ferricyanide
Reaction products	Sulfate, 2 Ferrocyt. <i>c</i>	Sulfate, 2 Ferrocyt. <i>c</i>	Sulfate, $H_2O_2$	Sulfate, 2 Ferrocyt. <i>c</i>	Sulfate, 2 Ferrocyt. <i>c</i>
Enzymatic mechanism	Ping-pong	Ping-pong	Ping-pong	Ping-pong	Ping-pong
References	[41]	[43]	[15, 47]	[6]	[7]

<sup>a</sup> Published  $k_{\text{cat}}$  numbers have been converted to turnover number for sulfite for consistency

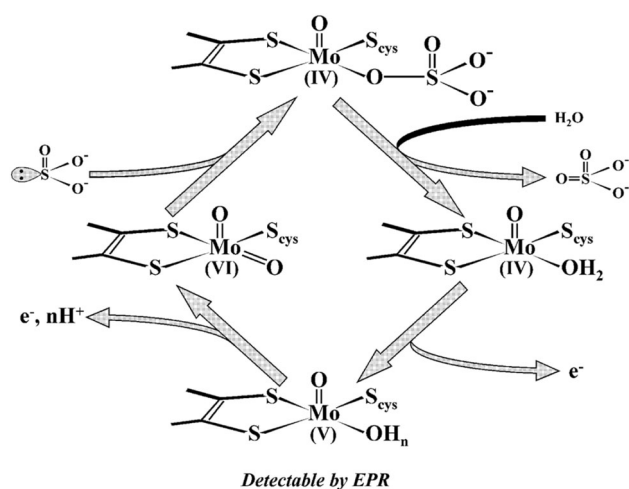


**Fig. 5** General view of Mo center oxidation state changes during turnover of SOEs. For PSO, molecular oxygen,  $O_2$ , is the electron acceptor, forming superoxide ion,  $[O_2]^-$ . Reproduced with permission from [56]

variants on the EPR spectra of these SOEs are described in a later section.

PSO and SorT are SOEs that contain a Mo center only. However, as noted above, the reoxidation of PSO by oxygen also proceeds by sequential one-electron transfers to form superoxide, which then nonenzymatically dismutates to hydrogen peroxide [18]. A simplified view of the catalytic cycle of the Mo-only SOEs is shown in Fig. 5.

All four SOEs that were discussed above have high affinities in the low micromolar range for their substrate, sulfite (Table 1), but their turnover numbers vary significantly. PSO, which interacts with an inorganic electron acceptor, has been reported to have a turnover number of  $4,500\text{ s}^{-1}$  [47], while the bacterial SorAB SDH that interacts with an external cytochrome  $c_{550}$  is able to catalyze  $\sim 350\text{ reactions s}^{-1}$  [6, 46]. Of the two vertebrate SOEs, HSO only catalyzes about 25 turnovers per second [43], whereas CSO has a turnover number of  $47\text{ s}^{-1}$  [41]. It has been suggested that the slower turnover rates for vertebrate SOEs might be due to the fact that the heme *b* domain of this enzyme has to reposition itself and ‘dock’ near the Mo site to be able to accept electrons from the Mo center [43]. However, laser flash photolysis measurements of the rate of IET between the Fe(II)/Mo(VI) and Fe(III)/Mo(V) states of CSO and HSO (IET #2 of Fig. 4) give respective first-order rate constants ( $k_{\text{et}}$  values) of  $1,318$  and  $491\text{ s}^{-1}$  [51]. These IET rates are much faster than the turnover rates and support facile interdomain motion that brings the heme and Mo centers close to one another [37]. The dependence of these  $k_{\text{et}}$  values upon viscosity provides experimental support for the hypothesis of interdomain motion in CSO and HSO [35]. However, there is no direct experimental study of interdomain motion. The Mo(VI/V)

potential is pH dependent [50], but at pH 7.5 the driving force for this IET #2 step in HSO is only  $\sim 20\text{ mV}$  [35]. It is ironic that SorAB SDH, in which the heme and Mo domains are locked into close proximity in the crystal structure, has a slower IET rate ( $k_{\text{et}} = 120\text{ s}^{-1}$ ) than either HSO or CSO [52]. HSO not only has the slowest turnover, but it also has the highest affinity for the substrate, sulfite, so a possibility is that substrate affinity has been optimized at the expense of catalytic turnover [53]. Another possibility is that rapid IET steps, but slow turnover in vertebrate SOEs may also reduce the production of toxic reactive oxygen species (ROS) in the mitochondria. Recent studies of HSO variants with truncated heme domains or shortened interdomain tethers exhibit increased reactivity with oxygen to give reactive oxygen products [54].

An interesting feature of the SOEs that interact with a mitochondrial-type cytochrome  $c_{550}$  (CSO/HSO, SorAB) is that the pH optimum of the reaction is close to pH 9, and the  $K_M$  sulfite values for these enzymes increase exponentially at pH values above 9 [6, 41, 43, 46]. In contrast, for the SorT sulfite dehydrogenase,  $K_M$  sulfite values were nearly invariant with pH in assays using ferricyanide as the electron acceptor [7]. Whether this is due to the use of a small molecule electron acceptor or is an inherent feature of this enzyme will have to be determined as so far no catalytic data for SorT in the presence of its natural electron acceptor, the SorU cytochrome, have been reported.

The implications of the absence of a second redox center for the enzyme mechanism are another point of interest. It is generally agreed that SOEs catalyze sulfite oxidation via a ping-pong mechanism, where a stable intermediate form of the enzymes (the sulfite reduced SOE) can be isolated. However, for SOEs that contain only a Mo cofactor, this stable state would be a Mo(IV), two-electron reduced enzyme, while for those enzymes that contain a heme redox center, the stable, reduced form of the enzyme would be a Mo(V) Fe(II) redox state (Fig. 4). This has direct implications for the use of spectroscopic techniques such as EPR that require a paramagnetic state of the Mo center. For the Mo center-only SOEs, intramolecular electron transfer steps are not possible, and the Mo(V) state becomes a highly transient intermediate of the oxidative half of the reaction cycle, rather than being the product of the reductive side of the reaction cycle (Fig. 5). Nevertheless, significant amounts of the Mo(V) state of Mo center-only SOEs can be generated for EPR studies, as described below for PSO. However, it is interesting that for SOEs it appears that the formation of the EPR-visible Mo(V) species occurs after the substrate oxidation reaction has been completed, i.e., the formation of the Mo(V) species is part of the oxidative part of the reaction cycle. This is different from other Mo enzymes, such as those of the xanthine oxidase

family, where Mo(V) is formed during interactions of the substrate with the Mo center [4].

### Catalytic cycle: details

#### Reaction at the molybdenum center

Figure 5 shows a representation of the proposed cycle for the oxidation of sulfite at the Mo center of SOEs [55, 56]. The dioxo-Mo(VI) resting state of the enzyme is shown on the left-hand side. Sulfite attacks the electrophilic equatorial oxo group to generate an oxo-Mo(IV)-sulfate intermediate (or transition state) shown at the top.

Hydrolysis releases the product (sulfate) and gives an oxo-Mo(IV)-aquo (or hydroxo) center (right-hand side). One-electron oxidation gives a paramagnetic oxo-Mo(V) center which gives characteristic EPR signals (Fig. 6). A second one-electron oxidation returns the Mo center to the oxidized Mo(VI) resting state.

For all the SOEs discussed here, the paramagnetic Mo(V) state depicted at the bottom of Fig. 5 is on the proposed catalytic pathway. For SorAB SDH and vertebrate SOEs, the first one-electron oxidation step involves transfer of an electron to the integral heme of the SOE, and the Mo(V) form can be generated by addition of excess sulfite to the oxidized Mo(VI) form of the protein in the absence of an exogenous oxidant required for turnover (Fig. 4). For PSO and variants of HSO which have no integral heme cofactor, the Mo(V) form can be generated

in vitro by reoxidation of the Mo(IV) form by addition of a substoichiometric amount of ferricyanide [57]. Thus, for all the SOEs discussed here, EPR spectroscopy has been a major tool for studying these enzymes over the years.

### Structures of the Mo(V) state of SOEs from EPR spectroscopy

X-ray crystal structures of SOEs (Fig. 3) provide a view of the overall organization of the enzymes as well as the coordination of the Mo center in the oxidized resting state. However, X-ray crystallography cannot specify the location of protons, which are important for understanding the catalytic mechanism. In addition, the molybdenum–sulfur centers of SOEs are prone to undergo photoreduction in the X-ray beam. Consequently, the observed X-ray intensities are from a time-dependent average of Mo oxidation states, which can hinder the elucidation of precise structural details of the Mo center.

The Mo(V) state of SOEs has a  $4d^1$  electron configuration, which is very favorable for study by EPR spectroscopy [58]. The diamagnetic Mo(VI) and Mo(IV) states are EPR silent, so only the Mo(V) state is detected by EPR spectroscopy, which makes the method well suited for studying transient Mo(V) species formed during the catalytic cycle. Interaction of the unpaired electron with nearby magnetic nuclei, including protons, can provide detailed structural information about the surroundings of the Mo center. Substitution of magnetically silent isotopes (e.g.,

**Fig. 6** Types of CW EPR spectra observed for SOEs and the corresponding structures for the Mo(V) centers deduced from electron spin echo (ESE) studies, isotopic labeling and density functional theory (DFT) calculations

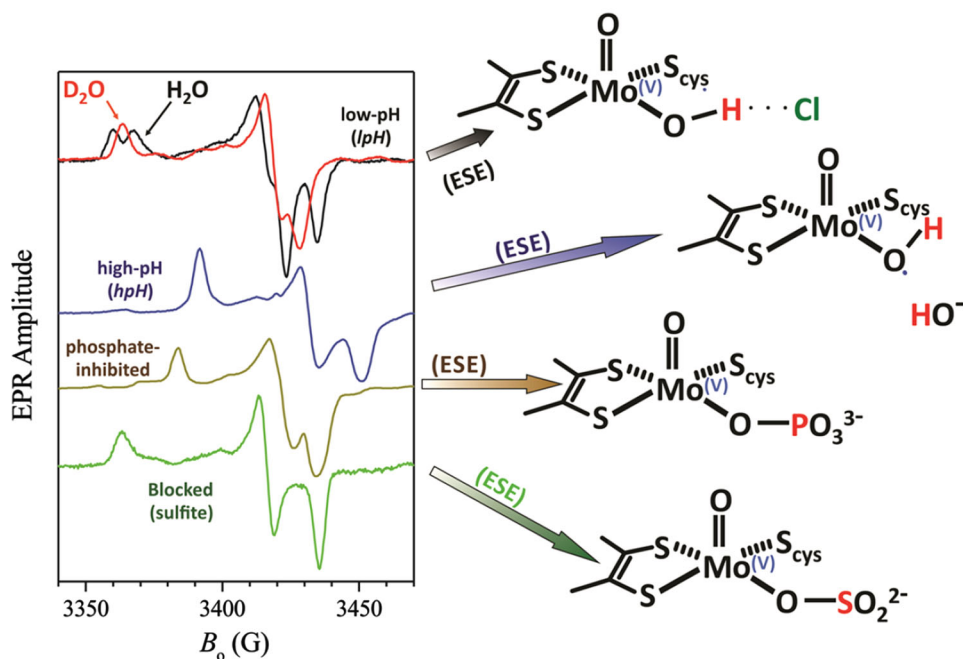


**Table 2** Types of CW EPR spectra observed for the Mo(V) states of SOEs

SOE	lpH	hpH	$P_i$	Sulfite (blocked)	References
SDH SorAB	No (Y236F) <sup>a</sup>	Yes	No	No (R55Q) <sup>a</sup>	[6, 46]
SDH SorT	n.r.	Yes	n.r.	n.r.	[40]
PSO	Minor <sup>b</sup>	Yes	No	Yes	[15, 60]
CSO and HSO	Yes	Yes	Yes	Yes	[59]

n.r. not reported

<sup>a</sup> Observed for this mutant

<sup>b</sup> minor component

<sup>16</sup>O and <sup>32</sup>S,  $I = 0$ ) with their magnetic counterparts (<sup>17</sup>O,  $I = 5/2$ ; <sup>33</sup>S,  $I = 3/2$ ) can provide additional insight regarding the structure of the Mo(V) center and intermediates in the catalytic cycle [59].

The first CW EPR spectra for a vertebrate SO (bovine) were reported in 1971 [61]. Four distinct types of CW EPR spectra (Fig. 6) have been identified based upon sensitivity to pH and anions: low pH (lpH), high pH (hpH), phosphate inhibited ( $P_i$ ) [62] and sulfite [63], more recently called “blocked” [59]. Table 2 summarizes which types of EPR spectra are observed for the different SOEs. The five-coordinate pseudo-square-pyramidal geometry about the Mo atom that is common to the SOEs (Fig. 1b) provides a framework for interpreting the EPR results. A recent review describes the use of variable-frequency pulsed EPR methods, isotopic labeling, synthesis of model compounds, and density functional theory (DFT) calculations to elucidate the structures on the right-hand side of Fig. 6 [59]. Here, we briefly summarize which EPR forms are observed for the various SOEs and describe the structures shown on the right side of Fig. 6. Errors by us and others in previously published structure assignments of the Mo(V) states of SOEs are also corrected.

**lpH form:** The lpH form is observed in CSO and recombinant human SO (HSO) at low pH ( $\leq 7.5$ ) and high chloride ( $\sim 100$  mM). The splitting in the CW EPR spectrum that collapses in D<sub>2</sub>O indicates an exchangeable proton, which was shown to be in the equatorial plane and probably hydrogen bonded to the coordinated cysteine by pulsed EPR spectroscopy [64] and DFT calculations [59]. Bray proposed that a chloride ion is associated with the Mo(V) site [65], and subsequently it was incorrectly assigned to be directly coordinated to the Mo atom, trans to the axial oxo group [66, 67]. However, extensive pulsed EPR studies using <sup>35,37</sup>Cl ( $I = 3/2$ ) isotopic labeling and DFT calculations on large models ( $>250$  atoms) showed that the Cl<sup>−</sup> ion is actually in the equatorial plane, hydrogen bonded to the equatorial OH ligand (as depicted

in Fig. 6) [68]. The observed <sup>35</sup>Cl<sup>−</sup> nuclear quadrupole coupling constant is small ( $\sim 3$  MHz) because the Cl<sup>−</sup> ion is in a nearly spherical environment of protons from water molecules and amino acid side chains. The lpH form is not observed in the SorAB SDH, even at [Cl<sup>−</sup>] = 200 mM [6], and PSO shows only minor amounts of the lpH form [15].

**hpH form:** The CW EPR spectra of CSO and HSO show no detectable splitting at high pH ( $>8$ ) and low chloride ( $\sim 1$  mM), but an exchangeable proton from a Mo–OH group was postulated [69]. A similar CW EPR spectrum is seen for PSO at high pH [15], and SorAB SDH shows the hpH spectrum at all pH values tested [6, 70]. Refocused primary echo experiments provided strong evidence for exchangeable protons in hpH CSO and HSO [64], and conclusive proof that the hpH form of SOEs contains exchangeable protons was provided by the primary ESEEM spectra of SorAB SDH, which show a frequency-dependent shift of the  $\nu_\sigma$  line for nearby protons [70]. The exchangeable protons in hpH SOEs have a large anisotropic hyperfine interaction and a very small ( $<1.5$  MHz) isotropic interaction, consistent with a coordinated –OH group that is rotated out of the equatorial plane containing the unpaired electron (Fig. 6), so that the O–H bond is nearly parallel to the terminal Mo=O bond [59]. The coordinated –OH group may also be weakly hydrogen bonded to a nearby water molecule or hydroxide ion [64].

**$P_i$  form:** Phosphate and other anions are inhibitors of HSO and CSO [41, 71]. Although the CW EPR spectrum at low pH in the presence of phosphate shows no observable hyperfine interaction with <sup>31</sup>P ( $I = 1/2$ , 100 % abundant), 1D [72] and 2D [59] pulsed EPR experiments clearly show <sup>31</sup>P hyperfine coupling, consistent with the coordination of phosphate via an oxygen, as shown in Fig. 6. No  $P_i$  form is observed for PSO or SorAB SDH.

**Sulfite (blocked) form:** In 1982 Bray and coworkers reported a sulfite form of CSO that was produced at low pH, but had no proton splitting [63]. PSO has a similar CW EPR at low pH with little or no proton splitting [15], and it was hypothesized that the product (sulfate) remained bound to the Mo(V) center [73]. Pulsed EPR studies of PSO that had been reduced with sulfite labeled with <sup>33</sup>S ( $I = 3/2$ ) showed hyperfine and nuclear quadrupole interactions for <sup>33</sup>S, consistent with the proposal of bound sulfate, although the nuclear quadrupole coupling constant ( $\sim 40$  MHz) seemed unusually large for <sup>33</sup>S in the tetrahedral environment of sulfate [60]. Similar <sup>33</sup>S parameters were obtained for the fatal R160Q mutant of HSO [74], for wt HSO and other HSO mutants reduced by <sup>33</sup>S-labeled sulfite in the absence of chloride [75], and for the analogous R55Q mutant of SorAB SDH [76]. In all of these cases, it was suggested that the active site was “blocked” by bound sulfate. However, more extensive DFT calculations on larger active site models for R160Q HSO showed

that the  $^{33}\text{S}$  nuclear quadrupole coupling constants were much more consistent with coordinated sulfite than coordinated sulfate [77]. The large excess of sulfite ( $\sim 20$ -fold) present in the reaction mixture leads to the species with coordinated sulfite being the dominant EPR form under the conditions of low pH and low chloride. Thus, the previous claims that the “blocked” form contains bound sulfate [60, 73–76] are incorrect. Rather, the so-called “blocked” form appears to be the sulfite form originally described by Bray and coworkers [63].

For wt CSO and HSO, the four different EPR forms shown in Fig. 6 and Table 2 can be interconverted by appropriate changes in pH and the concentrations of anions in the media. Mutations near the Mo active site can also profoundly affect the EPR forms that are observed and their distribution with pH. The best example of this is the conserved active site tyrosine residue (Y322 in CSO; Y343 in HSO; Y236 in SorAB SDH, Y267 in SorT SDH). For Y236F in SorAB SDH, the EPR spectra become pH dependent and both lpH and hpH forms are seen [78], which contrasts with SorABwt SDH, where only the hpH form is observed over the entire pH range [6]. For the Y343F HSO variant, the sulfite (“blocked”) form is observed at low pH ( $\sim 7$ ). As the pH is raised, the typical lpH spectrum appears and still persists at pH  $\sim 10$ , where a mixture of lpH and hpH forms is seen [79].

Mo(V) is proposed to be on the catalytic pathway for SOEs (Figs. 4, 5). The exquisite sensitivity of EPR spectroscopy, especially pulsed EPR methods, to relatively small changes in the immediate surroundings of the paramagnetic Mo(V) centers of SOEs provides a powerful tool for elucidating the intimate structures of their Mo(V) centers and for evaluating proposed catalytic mechanisms.

### Conclusions and future directions

SOEs have been characterized from bacterial, plant, and vertebrate sources. The enzymes have the same geometry about the Mo center (Fig. 1b), contain the same PPT cofactor (Fig. 1a), and involve the same sequence of oxidation state changes at the catalytic Mo center during turnover (Fig. 5). Pulsed EPR spectroscopy is a powerful tool for investigating the detailed structure of the paramagnetic Mo(V) center of the catalytic cycle and its interaction with substrates and inhibitors (Fig. 6). Although the physiological roles, quaternary protein structures, and overall catalytic reaction sequences differ among the three types of SOEs, their common role appears to be the minimization of the concentration of toxic sulfite in the organism by oxidizing it to benign sulfate. How this is accomplished depends upon the region of the cell or organelle where the SOE is primarily located and the

biochemical nature of the reduced product formed by the catalytic enzymatic oxidation of sulfite. For SOEs that also contain an integral heme unit, the reaction of sulfite with the Mo(VI) center in the reductive part of the catalytic cycle is rate limiting [41], and there is evidence that the conserved active site tyrosine plays a key role in product release [43]. The subsequent electron transfer steps of the reductive and oxidative paths are much faster.

Considerable progress has been made in elucidating the overall electron flow and final reduced products for various SOEs in recent years. For example, PSO resides in the peroxisomes of plants and uses  $\text{O}_2$  as the electron acceptor for the oxidation of sulfite, producing superoxide and ultimately hydrogen peroxide [18]. However, HSO resides in the mitochondria, and the production of harmful reactive oxygen species must be minimized. Bacterial SOEs that have been characterized usually are found in the bacterial periplasm, i.e., outside the cytoplasm, but in a clearly aerobic environment, as most of the bacteria that contain SOEs grow by aerobic respiration. However, bacterial SOEs do not appear to react directly with oxygen as part of sulfite catalysis. One of the main challenges for future studies of SOEs lies in advancing our understanding of how the various adaptations of the basic SOE unit have evolved to suit different physiological requirements of the organisms from which the enzymes originate. Included in this challenge is understanding why certain inherited defects in HSO cause isolated sulfite oxidase deficiency with severe neonatal neurological problems and early death (Table S1) [26].

Another challenge is posed by two large groups of archaeal and bacterial enzymes (cd\_02107-02019) that belong to the sulfite oxidase family, but for which no physiological function has so far been established [2, 27]. It is unclear whether these enzymes can actually catalyze sulfite oxidation. However, the fact that these enzymes are widely distributed within bacterial and archaeal species indicates that an as-yet-undiscovered biological role for these enzymes exists.

The various studies of the diversity of enzymes in the SO family also indicate that there may be many more structural variations of SOEs still to be discovered, especially in many clades of SOE phylogenetic trees that are made up of uncharacterized bacterial enzymes with clear homologies to SorT and SorAB [2, 27, 28].

There is also evidence that future studies of sulfite oxidation may have to look further afield to identify novel types of SOEs. It has been known for some time that certain types of bacteria are capable of carrying out sulfite oxidation but lack genes encoding typical, SO family SOEs in their genomes, although in some cases a clear dependence of direct sulfite oxidation on the availability of molybdenum in the growth medium could be shown [80].

Prominent examples of such bacteria belong to both the marine *Roseobacter* clade, and to the purple sulfur bacteria [80–84]. In these bacteria, an enzyme of the DMSO (dimethylsulfoxide) reductase enzyme family, another superfamily of Mo enzymes, has recently been proposed to carry out sulfite oxidation [81, 85]. Like other DMSO reductase family enzymes, this protein is a complex of three subunits including a membrane anchor and might be transferring electrons to the cellular quinol pool rather than to a soluble cytochrome, thus potentially allowing for the conservation of more energy. At present, only limited data on the properties of such enzymes are available, but their characterization will certainly add a completely new angle to the study of SOEs in living organisms.

**Acknowledgments** JHE gratefully acknowledges many years of financial support from NIGMS for research on molybdenum enzymes (Grant GM-037773). We thank A. Belaidi and G. Schwarz for a preprint of Ref. [54] and Dr. Megan Maher for help with the preparation of Figs. 1 and 3 and for a preprint of Ref. [40].

## References

- Frausto da Silva JJR, Williams RJP (2001) The biological chemistry of the elements—the inorganic chemistry of life. Oxford University Press, Oxford
- Kappler U (2011) *Biochim Biophys Acta* 1807:1–10
- Rajagopalan KV, Coughlan MP (1980) Molybdenum and molybdenum-containing enzymes. Pergamon Press, Oxford, pp 243–272
- Hille R, Hall J, Basu P (2014) *Chem Rev* 114:3963–4038
- Di Salle A, D’Errico G, La Cara F, Cannio R, Rossi M (2006) *Extremophiles* 10:587–598
- Kappler U, Bennett B, Rethmeier J, Schwarz G, Deutzmann R, McEwan AG, Dahl C (2000) *J Biol Chem* 275:13202–13212
- Wilson JJ, Kappler U (2009) *Biochim Biophys Acta* 1787:1516–1525
- Denger K, Weinitschke S, Smits THM, Schleheck D, Cook AM (2008) *Microbiology* 154:256–263
- Myers JD, Kelly DJ (2005) *Microbiology* 151:233–242
- Lyric RM, Suzuki I (1969) *Can J Biochem* 48:334–343
- Charles AM, Suzuki I (1965) *Biochem Biophys Res Comm* 19:686–690
- D’Errico G, Di Salle A, La Cara F, Rossi M, Cannio R (2006) *J Bacteriol* 188:694–701
- Low L, Kilmartin JR, Bernhardt PV, Kappler U (2011) *Front Microbiol* 2:58. doi:10.3389/fmicb.2011.00058
- Robin S, Arese M, Forte E, Sarti P, Giuffre A, Soulimane T (2011) *J Bacteriol* 193:3988–3997
- Eilers T, Schwarz G, Brinkmann H, Witt C, Richter T, Nieder J, Koch B, Hille R, Hänsch R, Mendel RR (2001) *J Biol Chem* 276:46989–46994
- Leustek T, Saito K (1999) *Plant Physiol* 120:637–644
- Schwarz G, Mendel RR (2006) *Annu Rev Plant Biol* 57:623–647
- Byrne RS, Hänsch R, Mendel RR, Hille R (2009) *J Biol Chem* 284:35479–35484
- Cohen HJ, Becher-Lange S, Kessler DL, Rajagopalan KV (1972) *J Biol Chem* 247:7759–7766
- Griffith OW (1987) *Methods Enzymol* 143:366–376
- Johnson JL (2003) *Prenatal Diagn* 23:6–8
- Dublin AB, Hald JK, Wootton-Gorges SL (2002) *AJNR Am J Neuroradiol* 23:484–485
- Sass JO, Gunduz A, Araujo Rodrigues Funayama C, Korkmaz B, Dantas Pinto KG, Tuysuz B, Yanasse Dos Santos L, Taskiran E, de Fátima Turcato M, Lam C-W, Reiss J, Walter M, Yalcinkaya C, Camelo Junior JS (2010) *Brain Dev* 32:544–549
- Leimkuehler S, Wuebbens MM, Rajagopalan KV (2011) *Coord Chem Rev* 255:1129–1144
- Mendel RR (2013) *J Biol Chem* 288:13165–13172
- Johnson JL, Coyne KE, Garrett RM, Zabet M-T, Dorche C, Kisker C, Rajagopalan KV (2002) *Hum Mutat* 20:74–79
- Kappler U (2008) *Microbial sulfur metabolism*. Springer, Berlin, pp 151–169
- Workun GJ, Moquin K, Rothery RA, Weiner JH (2008) *Microbiol Mol Biol Rev* 72:228–248
- Schrader N, Fischer K, Theis K, Mendel RR, Schwarz G, Kisker C (2003) *Structure* 11:1251–1263
- Wilson HL, Wilkinson SR, Rajagopalan KV (2006) *Biochemistry* 45:2149–2160
- Kisker C, Schindelin H, Pacheco A, Wehbi WA, Garrett RM, Rajagopalan KV, Enemark JH, Rees DC (1997) *Cell* 91:973–983
- Pacheco A, Hazzard JT, Tollin G, Enemark JH (1999) *J Biol Inorg Chem* 4:390–401
- Southerland WM, Rajagopalan KV (1978) *J Biol Chem* 253:8753–8758
- Southerland WM, Winge DR, Rajagopalan KV (1978) *J Biol Chem* 253:8747–8752
- Feng CJ, Kedia RV, Hazzard JT, Hurley JK, Tollin G, Enemark JH (2002) *Biochemistry* 41:5816–5821
- Johnson-Winters K, Nordstrom AR, Emesh S, Astashkin AV, Rajapaksha A, Berry RE, Tollin G, Enemark JH (2010) *Biochemistry* 49:1290–1296
- Kappler U, Bailey S (2005) *J Biol Chem* 280:24999–25007
- Utesch T, Mroginski MA (2010) *J Phys Chem Lett* 1:2159–2164
- Reichenbecher W, Kelly DP, Murrell JC (1999) *Arch Microbiol* 172:387–392
- McGrath AP, Laming EM, Guss JM, Trewella J, Calmes B, Bernhardt PV, Hanson GR, Kappler U, Maher MJ submitted
- Brody MS, Hille R (1999) *Biochemistry* 38:6668–6677
- Qiu JA, Wilson HL, Rajagopalan KV (2012) *Biochemistry* 51:1134–1147
- Wilson HL, Rajagopalan KV (2004) *J Biol Chem* 279:15105–15113
- Kalimuthu P, Heath MD, Santini JM, Kappler U, Bernhardt PV (2014) *Biochim Biophys Acta* 1837:112–120
- Rapson TD, Kappler U, Hanson GR, Bernhardt PV (2011) *Biochim Biophys Acta* 1807:108–118
- Bailey S, Rapson T, Winters-Johnson K, Astashkin AV, Enemark JH, Kappler U (2009) *J Biol Chem* 284:2053–2063
- Hänsch R, Lang C, Riebeseel E, Lindigkeit R, Gessler A, Rennerberg H, Mendel RR (2006) *J Biol Chem* 281:6884–6888
- Hemann C, Hood BL, Fulton M, Hänsch R, Schwarz G, Mendel RR, Kirk ML, Hille R (2005) *J Am Chem Soc* 127:16567–16577
- Feng C, Wilson HL, Hurley JK, Hazzard JT, Tollin G, Rajagopalan KV, Enemark JH (2003) *Biochemistry* 42:12235–12242
- Spence JT, Kipke CA, Enemark JH, Sunde RA (1991) *Inorg Chem* 30:3011–3015
- Feng C, Wilson HL, Hurley JK, Hazzard JT, Tollin G, Rajagopalan KV, Enemark JH (2003) *J Biol Chem* 278:2913
- Feng CJ, Kappler U, Tollin G, Enemark JH (2003) *J Am Chem Soc* 125:14696–14697
- Bar-Even A, Noor E, Savir Y, Liebermeister W, Davidi D, Tawfik DS, Milo R (2011) *Biochemistry* 50:4402–4410
- Belaidi AA, Roeper J, Krizowski S, Schwarz G (2014) submitted for publication

55. Hille R (1994) *Biochim Biophys Acta* 1184:143–169
56. Enemark JH, Astashkin AV, Raitsimring AM (2006) *Dalton Trans* 29:3501–3514
57. Klein EL, Belaidi AA, Raitsimring AM, Davis AC, Krämer T, Astashkin AV, Neese F, Schwarz G, Enemark JH (2014) *Inorg Chem* 53:961–971
58. Mabbs FE, Collison D (1992) *Electron paramagnetic resonance of d transition metal complexes*. Elsevier, Amsterdam
59. Klein EL, Astashkin AV, Raitsimring AM, Enemark JH (2013) *Coord Chem Rev* 257:110–118
60. Astashkin AV, Johnson-Winters K, Klein EL, Byrne RS, Hille R, Raitsimring AM, Enemark JH (2007) *J Am Chem Soc* 129:14800–14810
61. Cohen HJ, Fridovich I, Rajagopalan KV (1971) *J Biol Chem* 246:374–382
62. Lamy MT, Gutteridge S, Bray RC (1980) *Biochem J* 185:397–403
63. Bray RC, Lamy MT, Gutteridge S, Wilkinson T (1982) *Biochem J* 201:241–243
64. Astashkin AV, Mader ML, Pacheco A, Enemark JH, Raitsimring AM (2000) *J Am Chem Soc* 122:5294–5302
65. Bray RC, Gutteridge S, Lamy MT, Wilkinson T (1983) *Biochem J* 211:227–236
66. Doonan CJ, Wilson HL, Bennett B, Prince RC, Rajagopalan KV, George GN (2008) *Inorg Chem* 47:2033–2038
67. Astashkin AV, Klein EL, Enemark JH (2007) *J Inorg Biochem* 101:1623–1629
68. Klein EL, Astashkin AV, Ganyushin D, Riplinger C, Johnson-Winters K, Neese F, Enemark JH (2009) *Inorg Chem* 48:4743–4752
69. George GN (1985) *J Magn Reson* 64:384–394
70. Raitsimring AM, Kappler U, Feng CJ, Astashkin AV, Enemark JH (2005) *Inorg Chem* 44:7283–7285
71. Sullivan EP, Hazzard JT, Tollin G, Enemark JH (1992) *J Am Chem Soc* 114:9662–9663
72. Pacheco A, Basu P, Borbat P, Raitsimring AM, Enemark JH (1996) *Inorg Chem* 35:7001–7008
73. Astashkin AV, Hood BL, Feng CJ, Hille R, Mendel RR, Raitsimring AM, Enemark JH (2005) *Biochemistry* 44:13274–13281
74. Astashkin AV, Johnson-Winters K, Klein EL, Feng CJ, Wilson HL, Rajagopalan KV, Raitsimring AK, Enemark JH (2008) *J Am Chem Soc* 130:8471–8480
75. Rajapakshe A, Johnson-Winters K, Nordstrom AR, Meyers KT, Emesh S, Astashkin AV, Enemark JH (2010) *Biochemistry* 49:5154–5159
76. Rapson TD, Astashkin AV, Johnson-Winters K, Bernhardt PV, Kappler U, Raitsimring AM, Enemark JH (2010) *J Biol Inorg Chem* 15:505–514
77. Klein EL, Raitsimring AM, Astashkin AV, Rajapakshe A, Johnson-Winters K, Arnold AR, Potapov A, Goldfarb D, Enemark JH (2012) *Inorg Chem* 51:1408–1418
78. Kappler U, Bailey S, Feng CJ, Honeychurch MJ, Hanson GR, Bernhardt PV, Tollin G, Enemark JH (2006) *Biochemistry* 45:9696–9705
79. Raitsimring AM, Astashkin AV, Feng C, Wilson HL, Rajagopalan KV, Enemark JH (2008) *Inorg Chim Acta* 361:941–946
80. Dahl C (1996) *Microbiology* 142:3363–3372
81. Lenk S, Moraru C, Hahnke S, Arnds J, Richter M, Kube M, Reinhardt R, Brinkhoff T, Harder J, Amann R, Mussmann M (2012) *ISME J* 6:2178–2187
82. Moran MA, Belas R, Schell MA, Gonzalez JM, Sun F, Sun S, Binder BJ, Edmonds J, Ye W, Orcutt B, Howard EC, Meile C, Palefsky W, Goesmann A, Ren Q, Paulsen I, Ulrich LE, Thompson LS, Saunders E, Buchan A (2007) *Appl Environ Microbiol* 73:4559–4569
83. Wagner-Döbler I, Biebl H (2006) *Annu Rev Microbiol* 60:255–280
84. Buchan A, Gonzalez JM, Moran MA (2005) *Appl Environ Microbiol* 71:5665–5677
85. Dahl C, Franz B, Hensen D, Kesselheim A, Zigann R (2013) *Microbiology* 159:2626–2638